

Vincent K. S. Hsiao

Department of Applied Materials and
Optoelectronic Engineering,
National Chi Nan University,
Nantou, 54561 Taiwan;
Department of Engineering Science and
Mechanics,
The Pennsylvania State University,
University Park, PA 16802
e-mail: khsiao@ncnu.edu.tw

Yue Bing Zheng

Department of Engineering Science and
Mechanics,
The Pennsylvania State University,
University Park, PA 16802
e-mail: yzz113@gmail.com

Heike Betz

The Huck Institutes of the Life Science,
The Pennsylvania State University,
University Park, PA 16802
e-mail: hsb6@psu.edu

Brian Kiraly

e-mail: btk5051@psu.edu

Wei Yan

e-mail: wyan.nc@gmail.com

Department of Engineering Science and
Mechanics,
The Pennsylvania State University,
University Park, PA 16802

Pamela F. Lloyd

e-mail: pamela.lloyd@wpafb.af.mil

Timothy J. Bunning

e-mail: timothy.bunning@wpafb.af.mil

Materials and Manufacturing Directorate,
Air Force Research Laboratory,
Wright-Patterson Air Force Base,
Dayton, OH 45433

Alexander N. Cartwright

Institute for Lasers, Photonics and Biophotonics,
University at Buffalo,
The State University of New York,
Buffalo, NY 14260-3000
e-mail: anc@buffalo.edu

Tony Jun Huang

Department of Engineering Science and
Mechanics,
The Pennsylvania State University,
University Park, PA 16802
e-mail: junhuang@psu.edu

Holographically Fabricated Dye-Doped Nanoporous Polymers as Matrix for Laser Desorption/ Ionization Mass Spectrometry

We report laser desorption/ionization mass spectrometry using a dye-doped nanoporous polymer matrix. The nanoporous polymer matrix was fabricated through a holographic interference patterning technique. The periodically aligned nanopores in the resulting polymer matrix produced a high surface-to-volume ratio that facilitates the homogeneous cocrystallization of the matrix and an analyte (i.e., peptide in this demonstration). To generate nanostructures with further enhanced functionalities, dyes were also incorporated into the photopolymer. We demonstrate that by using the dye-doped nanoporous polymer matrix, we can identify peptides with an enhanced signal from the peptides and decreased noise from the ion fragmentation. These results indicate that the dye-doped nanoporous polymer matrix we use here can be a promising platform for laser desorption/ionization mass spectrometry. [DOI: 10.1115/1.4002610]

Manuscript received September 8, 2010; final manuscript received September 21, 2010; published online October 29, 2010. Editor: Vijay K. Varadan.

1 Introduction

Matrix-assisted laser desorption/ionization (MALDI) is an important ionization technique used in mass spectrometry, allowing for the analysis of both organic molecules (such as polymers) and biomolecules (such as proteins, peptides, and nucleic acids) [1–7]. To generate a strong MALDI signal necessary for mass spectrometry, a matrix (a small molecule with a molecular weight (MW) ranging from 150 to 250) is often used to activate the ionization process of the analytes. As the matrix absorbs photons from a laser, the efficient energy transfer from the matrix to the analyte causes the analyte to ionize. The resulting ionized analyte desorbs from the substrate and is subsequently detected by the mass spectrometer. As of this moment, MALDI has not been extensively used in mass spectrometry applications. Besides its complex sample preparation process, another major obstacle that prevents MALDI from realizing its potential is the significant ion fragmentation and interference caused by the large molar ratio of the organic matrix to the analyte. This hinders traditional MALDI techniques from effectively identifying analytes with small molecular weights (<1800) [8,9].

To date, several methods have been developed to simplify the complex sample preparation process and reduce background interference generated by traditional MALDI techniques. A matrix-free mass spectrometry technique, known as desorption/ionization on porous silicon (DIOS), has been experimentally demonstrated to detect small molecules with little or no interference [10–14]. In the DIOS method, porous silicon allows the analyte to absorb UV light, vaporize, and subsequently ionize through a photoluminescence process. Alternatively, ion fragmentation can be reduced by fabricating a porous polymer monolith, which uses a polymerization or sol-gel process to entrap the organic matrix on the polymeric substrate [15–21]. The integrated organic matrix offers sufficient energy transfer from the matrix-modified substrate to the analyte, thus enabling the identification of small-molecule analytes. The interference is diminished due to the covalent bonding between the matrix and the polymeric substrate. Other alternative approaches, such as carbon-based polymers, carbon nanotubes, and metal nanoparticles, have also been demonstrated to decrease ion fragmentation and improve the detection capability of analytes with small molecular weights [22–28].

In this article, we demonstrate that a dye-doped nanoporous polymer matrix can be developed and used to detect small molecules (peptides, molecular weight: ~1570). The polymeric nanostructures, fabricated by a laser holographic patterning technique, have been established in applications such as biosensing and humidity sensing [29–35] and are emerging as functional materials for nanophotonics [36–47]. In this work, we successfully functionalize the polymeric nanostructure with a fluorescent dye (Coumarin 456) and trifluoroacetic acid. We further prove that this dye-doped nanoporous polymeric structure can be used as a matrix in laser desorption/ionization applications with marginal background interference. In addition to decreasing the background interference in the laser desorption/ionization process, this dye-doped nanoporous polymer simplifies sample preparation.

2 Experimental Details

Rose Bengal (RB), N-phenylglycine (NPG), N-vinylpyrrolidinone (NVP), dipentaerythritol hydroxypenta acrylate (DPHPA), acetone, acetonitrile, high-performance liquid chromatography (HPLC)-grade water, trifluoroacetic acid, and peptide ([Glu¹]-fibrinopeptide B human, MW 1570.57) were purchased from Aldrich (Milwaukee, WI) for use in the experiments. The fluorescent dye, Coumarin 456 (C456), was purchased from Exciton (Dayton, OH) and the liquid crystal (TL213) from Merck Ltd. All chemicals were used without further purification.

The dye-doped nanoporous polymer matrix was fabricated by a holographic interference patterning process [29,30]. Two 514 nm laser beams, separated from an argon ion laser source (Coherent

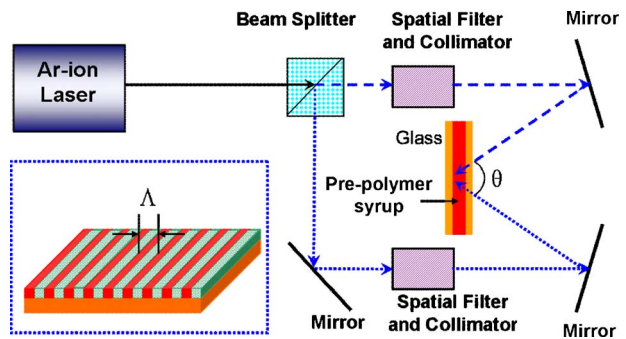


Fig. 1 Schematic of the optical setup for fabricating one-dimensional, nanoporous polymer

Innova 300C), generated periodically dispersed high and low intensity regions. The schematic of our fabrication setup is shown in Fig. 1. The prepolymer syrup, consisting of monomer (40 wt % DPHPA), photoinitiator (1 wt % RB), co-initiator (3 wt % NPG), dye (4 wt % C456), homogenizer (20 wt % NVP), nonreactive solvent (15 wt % acetone), liquid crystal (15 wt % TL213), and acid (2 wt % trifluoroacetic acid), was homogeneously mixed before laser exposure. The cell was prepared by positioning 10 μ l of prepolymer syrup onto the top of one glass slide, which was immediately covered by another glass slide. The thickness of the sandwiched polymer syrup was controlled by 5 μ m glass rods mixed within the prepolymer syrup. After holographic interference patterning, the sandwiched cell was post-cured under a 100 W halogen lamp for 24 h. The laser writing angle (θ), power, time, and exposure area were fixed at 20 deg, 100 mW, 1 min, and 20 \times 20 mm², respectively. The control sample (“nonporous” polymer doped with dye and trifluoroacetic acid) was prepared using a similar preparation procedure except only one laser beam was used for laser exposure. A scanning electron microscope (SEM, Hitachi S-5200) was used to examine the surface and cross-sectional morphology of the polymeric nanostructures.

The MALDI preparation process began by preparing a matrix (C456) at a concentration of 10 mg/ml dissolved in 50% acetonitrile and 0.1% trifluoroacetic acid in HPLC water on a stainless steel plate (Waters, M880675CD1-S). The analyte and matrix were mixed at a 1:1 ratio, and 2 μ l mixture was spotted onto the stainless steel plate. The analyte/matrix spots were set to air-dry for 30 min at room temperature before the MALDI analysis was performed.

The MALDI analysis was conducted using a MALDI–time of flight (TOF) LR instrument (Waters, Ltd.). The analyte for the dye-doped nanoporous polymer matrix was prepared by dissolving the peptide in HPLC water (50 pmol/ μ l). The peptide solution was diluted (1:1) with acetonitrile. A 2 μ l diluted peptide solution was applied directly onto the top of the polymeric nanostructure and set to air-dry for 1 min. The experimental conditions for laser desorption/ionization (LDI) were set to the positive-ion reflection mode with a pulse voltage of 2300 V, a source voltage of 15 kV, a reflection voltage of 2000 V, and a multi-channel plate (MCP) detector voltage of 1950 V. The sampling period was 0.5 ns with a time-lag focusing (TLF) delay of 500 ns. Ten shots per spectrum were taken with a laser firing rate of 5 Hz.

3 Results and Discussion

The formation of periodically arranged nanopores strongly depends on the degree of phase separation during the photopolymerization process. The addition of a nonreactive solvent (i.e., acetone) into the prepolymer syrup is key to the formation of nanopores in the structure. During the photopolymerization process, the solvent phase-separated from the photopolymer to form

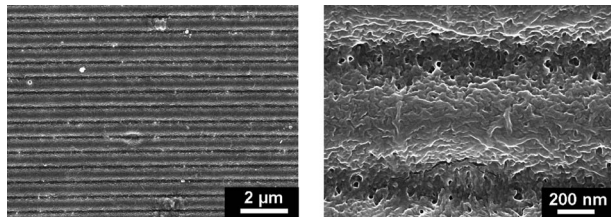


Fig. 2 Surface morphology of the nanoporous polymer functionalized with C456 and trifluoroacetic acid, characterized by SEM

nanoscale droplets. After the droplets of solvent evaporated, nanoscale air voids were left in the polymer structure, forming periodic nanoporous polymeric structures.

Figure 2 depicts the surface morphology of the nanoporous polymers, which clearly reveals the alternating layers of polymer and void strips. The period of the grating, calculated to be 800 nm, corresponds to the total widths of nonporous regions (600 nm) and porous regions (200 nm). The voids (10–100 nm in diameter) in the porous regions create a high surface-to-volume ratio, facilitating the ionization and desorption of the analytes.

Figure 3 shows an experimental schematic of the LDI measurement based on the dye-doped nanoporous polymeric structures. The fabricated nanostructure, situated on a glass substrate, was set in a custom-made plate with dimensions similar to those of conventional MALDI stainless steel plates. During laser irradiation, the dye-doped nanoporous polymer sample absorbs energy from the laser and efficiently ionizes the analyte because of the polymer's large surface-to-volume ratio. In a strong electric field, the ionized analyte accelerates into a flight tube attached to a detector. By recording the flight time of the ionized analyte, the mass of the analyte can be calculated. The mass to charge ratio (m/z) is determined by the amount of kinetic energy applied to the analyte throughout the flight tube [1].

To demonstrate that the dye-doped nanoporous polymers can achieve improved MALDI signal with decreased interference (i.e., noise), we carried out several experiments. In the first experiment, we performed mass spectrometry of a peptide ([Glu¹]-fibrinopeptide B human) using a traditional dye (C456) matrix. As seen in Fig. 4(a), while a peak at 1570.60 m/z accurately represents the molecular weight of the peptide, various

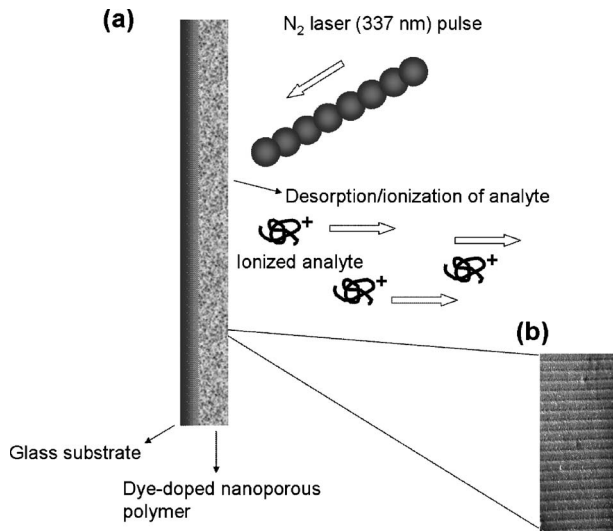


Fig. 3 (a) Experimental setup for dye-doped nanoporous polymer-assisted LDI spectrometry. (b) Cross-sectional morphology of dye-doped nanoporous polymer.

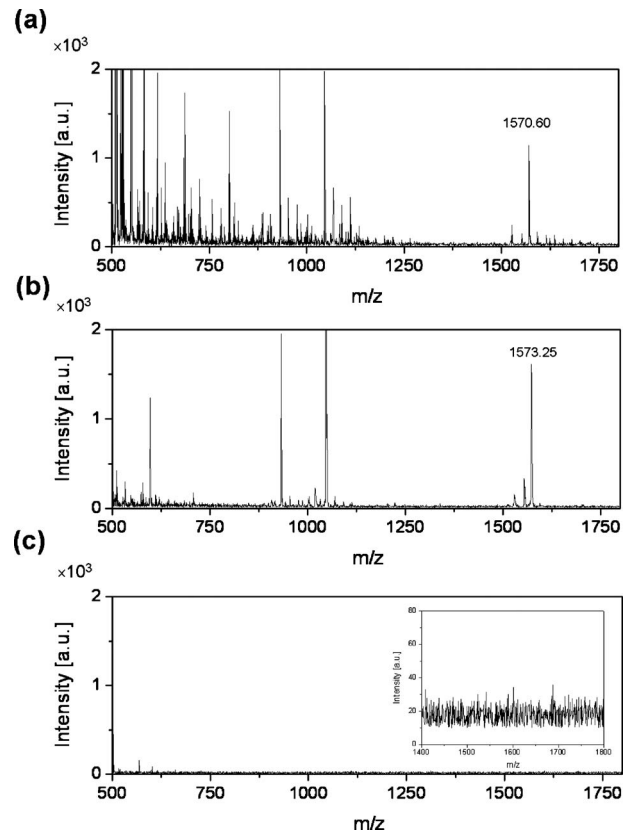


Fig. 4 Mass spectra of [Glu¹]-fibrinopeptide B human (MW 1570.57) obtained by using (a) nanoporous polymer film doped with C456, (b) nanoporous polymer film doped with C456 and trifluoroacetic acid, and (c) nonporous polymer film doped with C456 and trifluoroacetic acid. The inset shows the enlarged high mass region from 1400 to 1800 m/z .

peaks between 500 and 1100 m/z were observed. These interference peaks (500–1100 m/z) arose from ion fragmentation due to the large molar ratio of the dye, limiting the application range of the dye matrix [2]. In the second experiment, we performed mass spectrometry of the peptide using a nanoporous polymer matrix functionalized with C456 and trifluoroacetic acid. As seen in Fig. 4(b), the peptide signal remained strong while the interference at the low m/z region significantly decreased. In the third set of experiments, we performed mass spectrometry of peptide using a control sample, a nonporous polymer matrix functionalized with C456 and trifluoroacetic acid. As seen in Fig. 4(c), no peptide signal was observed, indicating that nanopores play a vital role in the enhanced mass analysis of peptide.

To examine the role of the C456 dye in the dye-doped nanoporous polymer, we carried out another control experiment. Figure 5(a) shows the mass spectrum of peptide using nanoporous polymer without doping the C456 dye. It indicates that no peptide signal was observed. Unlike DIOS-mass spectrometry (MS), where analytes directly absorb UV light, the undoped nanostructure used here has no absorption in the UV range, making it impossible to transfer the photon energy to the peptide. Thus, the incorporation of dyes into the nanoporous polymeric structures is essential in performing MALDI functions. We believe that the high surface-to-volume ratio of nanostructures can facilitate the formation of cocrystallized matrix/analyte compounds with a low molar ratio of dye.

We further examined the role of trifluoroacetic acid in the dye-doped nanoporous polymer. Figure 5(b) shows the mass spectrum of peptide using a dye-doped nanoporous polymer that does not contain trifluoroacetic acid. It reveals a weak peptide signal com-

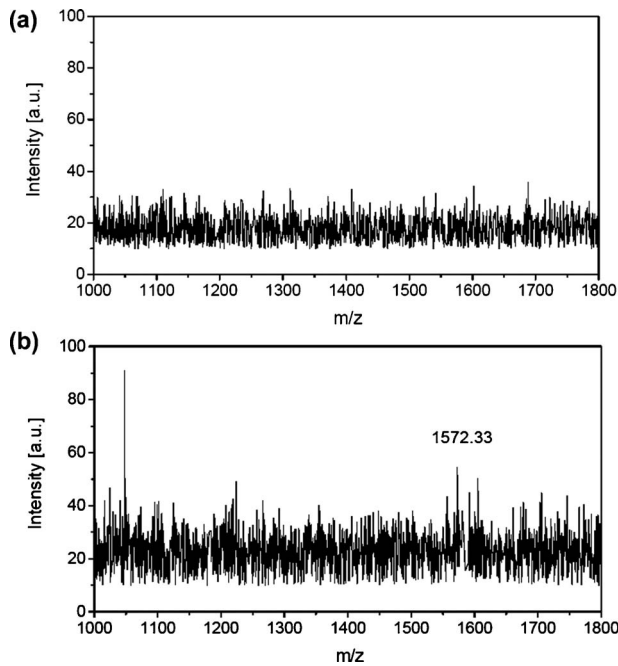


Fig. 5 Mass spectra of control samples. (a) Mass spectra of peptide using nanoporous polymer film that does not contain C456. (b) Mass spectra of peptide using C456-doped nanoporous polymer film that does not contain trifluoroacetic acid.

pared with the signal from a dye-doped nanoporous polymer that contains trifluoroacetic acid (Fig. 4(b)). In traditional MALDI essays, trifluoroacetic acid has proven to be an effective acid in increasing the cocrystallization between matrix and analyte, greatly enhancing the analyte signal [4]. Figure 6 compares surface morphology of the nanoporous polymer functionalized with trifluoroacetic acid before (Fig. 6(a)) and after (Fig. 6(b)) adding the peptide solution. Figure 6(a) reveals an empty, weblike morphology of the void strips before depositing the analyte solution, while Fig. 6(b) clearly indicates that the areas of the void strip are filled with small particlelike nanostructures. We speculate that the nanopores promote the peptide solution to cocrystallize with the matrix in the porous regions. With this approach, different kinds of chemical modifiers can be dissolved and incorporated into the photopolymer to facilitate the fabrication of nanoporous structures with tailored functionalities. In our experiments, we functionalized the porous polymer structures with trifluoroacetic acid to improve the LDI signal, and we will further optimize the recipe of the dye-doped nanoporous polymer (e.g., the concentration of trifluoroacetic acid) to improve the LDI signals.

4 Conclusions

Using a holographic lithography method, we have successfully fabricated a dye-doped nanoporous polymer and demonstrated

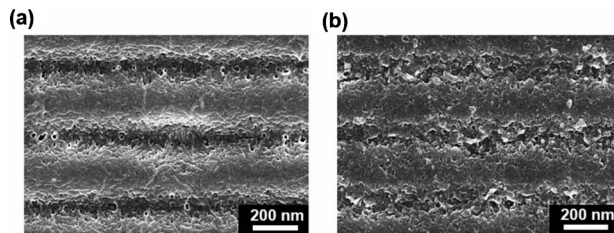


Fig. 6 Surface morphology of the nanoporous polymer film doped with C456 and trifluoroacetic acid (a) before and (b) after adding peptide onto the top of the film

that this dye-doped nanoporous polymer can be used as a platform for LDI analysis. In the LDI analysis, the dye served as a modifier to the photopolymer to facilitate the photon energy transformation between the matrix and the analyte. The high surface-to-volume ratio of the nanoporous polymer facilitates the photon energy transformation and enhances the LDI signal. Moreover, the primary drawbacks of traditional MALDI analysis (i.e., background interference and ion fragmentation) were circumvented in this approach due to the low molar ratio of the dye component in the cocrystallized matrix/analyte compound. We expect that with these advantages, the dye-doped nanoporous polymer matrix described here will be a promising technology for future LDI mass spectrometry.

Acknowledgment

This research was supported by U.S. Department of Agriculture (USDA/NRI), Air Force Office of Scientific Research (US-AFOSR), National Science Foundation (NSF), the Penn State Centre for Nanoscale Science (MRSEC), and the National Science Council, Taiwan (Grant No. NSC 98-2221-E260-001). Components of this work were conducted at the Penn State node of the NSF-funded National Nanotechnology Infrastructure Network.

References

- [1] Karas, M., and Bahr, U., 1991, "Matrix-Assisted Laser Desorption/Ionization Mass Spectrometry," *Mass Spectrom. Rev.*, **10**, pp. 335–357.
- [2] Fitzgerald, M. C., Parr, G. R., and Smith, L. M., 1993, "Basic Matrixes for the Matrix-Assisted Laser Desorption/Ionization Mass Spectrometry of Proteins and Oligonucleotides," *Anal. Chem.*, **65**, pp. 3204–3211.
- [3] Gusev, A., Vasseur, O., Proctor, A., Sharkey, A. G., and Hercules, D. M., 1995, "Imaging of Thin-Layer Chromatograms Using Matrix-Assisted Laser Desorption/Ionization Mass Spectroscopy," *Anal. Chem.*, **67**, pp. 4565–4570.
- [4] Harvey, D., 1999, "Matrix-Assisted Laser Desorption/Ionization Mass Spectrometry of Carbohydrates," *Mass Spectrom. Rev.*, **18**, pp. 349–450.
- [5] Mehl, J. T., and Hercules, D. M., 2000, "Direct TLC-MALDI Coupling Using a Hybrid Plate," *Anal. Chem.*, **72**, pp. 68–73.
- [6] Lewis, J. K., Wei, J., and Siuzdak, G., 2000, *Encyclopedia of Analytical Chemistry*, Wiley, New York, p. 5894.
- [7] Dreisewerd, K., Koelbl, S., Peter-Katalinic, J., Berkenkamp, S., and Pohlentz, G. J., 2006, "Analysis of Native Milk Oligosaccharides Directly From Thin-Layer Chromatography Plates by Matrix-Assisted Laser Desorption/Ionization Orthogonal-Time-of-Flight Mass Spectrometry With a Glycerol Matrix," *J. Am. Soc. Mass Spectrom.*, **17**, pp. 139–150.
- [8] Peterson, D. S., 2007, "Matrix-Free Methods for Laser Desorption/Ionization Mass Spectrometry," *Mass Spectrom. Rev.*, **26**, pp. 19–34.
- [9] Kim, Y., Hurst, G. B., Doktycz, M. J., and Buchanan, M. V., 2001, "Improving Spot Homogeneity by Using Polymer Substrates in Matrix-Assisted Laser Desorption/Ionization Mass Spectrometry of Oligonucleotides," *Anal. Chem.*, **73**, pp. 2617–2624.
- [10] Wei, J., Buriak, J. M., and Siuzdak, G., 1999, "Desorption-Ionization Mass Spectrometry on Porous Silicon," *Nature (London)*, **399**, pp. 243–246.
- [11] Shen, Z. X., Thomas, J. J., Averbuj, C., Broo, K. M., Engelhard, M., Crowell, J. E., Finn, M. G., and Siuzdak, G., 2001, "Porous Silicon as a Versatile Platform for Desorption/Ionization Mass Spectrometry," *Anal. Chem.*, **73**, pp. 612–619.
- [12] Chen, Y.-C., and Wu, J.-Y., 2001, "Analysis of Small Organics on Planar Silica Surfaces Using Surface-Assisted Laser Desorption/Ionization Mass Spectrometry," *Rapid Commun. Mass Spectrom.*, **15**, pp. 1899–1903.
- [13] Tuomikoski, S., Huikko, K., Grigoras, K., Ostman, P., Kostianen, R., Baumann, M., Abian, J., Kotiaho, T., and Franssila, S., 2002, "Preparation of Porous n-Type Silicon Sample Plates for Desorption/Ionization on Silicon Mass Spectrometry (DIOS-MS)," *Lab Chip*, **2**, pp. 247–253.
- [14] Gorecka-Drzazga, A., Bargiel, S., Walczak, R., Dziuban, J. A., Kraj, A., Dy-lag, T., and Sillberring, J., 2004, "Desorption/Ionization Mass Spectrometry on Porous Silicon Dioxide," *Sens. Actuators B*, **103**, pp. 206–212.
- [15] Hauck, H. E., and Schulz, M., 2002, "Ultrathin-Layer Chromatography," *J. Chromatogr. Sci.*, **40**, pp. 550–552.
- [16] Salo, P. K., Salomies, H., Harju, K., Ketola, R. A., Kotiaho, T., Yil-Kauhaluoma, J. I., and Kostianen, R., 2005, "Analysis of Small Molecules by Ultrathin-Layer Chromatography-Atmospheric Pressure Matrix-Assisted Laser Desorption/Ionization Mass Spectrometry," *J. Am. Soc. Mass Spectrom.*, **16**, pp. 906–915.
- [17] Peterson, D. S., Luo, Q., Hilder, E. F., Svec, F., and Frechet, J. M. J., 2004, "Porous Polymer Monolith for Surface-Enhanced Laser Desorption/Ionization Time-of-Flight Mass Spectrometry of Small Molecules," *Rapid Commun. Mass Spectrom.*, **18**, pp. 1504–1512.
- [18] Bakry, R., Bonn, G. K., Mair, D., and Svec, F., 2007, "Monolithic Porous Polymer Layer for the Separation of Peptides and Proteins Using Thin-Layer Chromatography Coupled With MALDI-TOF-MS," *Anal. Chem.*, **79**, pp. 486–493.

- [19] Lin, Y. S., and Chen, Y. C., 2002, "Laser Desorption/Ionization Time-of-Flight Mass Spectrometry on Sol-Gel-Derived 2,5-Dihydroxybenzoic Acid Film," *Anal. Chem.*, **74**, pp. 5793–5798.
- [20] Teng, C. H., and Chen, Y. C., 2003, "Fiber Introduction Mass Spectrometry: Coupling Solid-Phase Microextraction With Sol-Gel-Assisted Laser Desorption/Ionization Time-of-Flight Mass Spectrometry," *Rapid Commun. Mass Spectrom.*, **17**, pp. 1092–1094.
- [21] Chen, C. T., and Chen, Y. C., 2004, "Molecularly Imprinted TiO₂-Matrix-Assisted Laser Desorption/Ionization Mass Spectrometry for Selectively Detecting α -Cyclodextrin," *Anal. Chem.*, **76**, pp. 1453–1457.
- [22] Sunner, J., Dratz, E., and Chen, Y. C., 1995, "Graphite Surface-Assisted Laser Desorption/Ionization Time-of-Flight Mass Spectrometry of Peptides and Proteins From Liquid Solutions," *Anal. Chem.*, **67**, pp. 4335–4342.
- [23] O'Donnell, M. J., Tang, K., Kolster, H., Smith, C. L., and Cantor, C. R., 1997, "High-Density, Covalent Attachment of DNA to Silicon Wafers for Analysis by MALDI-TOF Mass Spectrometry," *Anal. Chem.*, **69**, pp. 2438–2443.
- [24] Xu, S., Li, Y., Zou, H., Qiu, J., Guo, Z., and Guo, B., 2003, "Carbon Nanotubes as Assisted Matrix for Laser Desorption/Ionization Time-of-Flight Mass Spectrometry," *Anal. Chem.*, **75**, pp. 6191–6195.
- [25] Sudhir, P., Wu, H. F., and Zhou, Z. C., 2005, "Identification of Peptides Using Gold Nanoparticle-Assisted Single-Drop Microextraction Coupled With AP-MALDI Mass Spectrometry," *Anal. Chem.*, **77**, pp. 7380–7385.
- [26] Teng, C. H., Ho, K. C., Lin, Y. S., and Chen, Y. C., 2004, "Gold Nanoparticles as Selective and Concentrating Probes for Samples in MALDI MS Analysis," *Anal. Chem.*, **76**, pp. 4337–4342.
- [27] Ren, S., and Guo, Y., 2005, "Oxidized Carbon Nanotubes as Matrix for Matrix-Assisted Laser Desorption/Ionization Time-of-Flight Mass Spectrometric Analysis of Biomolecules," *Rapid Commun. Mass Spectrom.*, **19**, pp. 255–260.
- [28] Castellana, E. T., and Russell, D. H., 2007, "Tailoring Nanoparticle Surface Chemistry to Enhance Laser Desorption Ionization of Peptides and Proteins," *Nano Lett.*, **7**, pp. 3023–3025.
- [29] Hsiao, V. K. S., Kirkey, W. D., Chen, F., Cartwright, A. N., Prasad, P. N., and Bunning, T. J., 2005, "Organic Solvent Vapor Detection Using Holographic Photopolymer Reflection Gratings," *Adv. Mater.*, **17**, pp. 2211–2214.
- [30] Hsiao, V. K. S., Lin, T. C., He, G. S., Cartwright, A. N., Prasad, P. N., Natarajan, L. V., Tondiglia, V. P., and Bunning, T. J., 2005, "Optical Microfabrication of Highly Reflective Volume Bragg Gratings," *Appl. Phys. Lett.*, **86**, p. 131113.
- [31] Maskaly, K. R., Hsiao, V. K. S., Cartwright, A. N., Prasad, P. N., Lloyd, P. F., Bunning, T. J., and Carter, W. C., 2006, "Experimental Verification of the Applicability of the Homogenization Approximation to Rough One-Dimensional Photonic Crystals Using a Holographically Fabricated Reflection Grating," *J. Appl. Phys.*, **100**, p. 066103.
- [32] Shi, J., Hsiao, V. K. S., Walker, T. R., and Huang, T. J., 2008, "Humidity Sensing Based on Nanoporous Polymeric Photonic Crystals," *Sens. Actuators B*, **129**, pp. 391–396.
- [33] Hsiao, V. K. S., Waldeisen, J. R., Zheng, Y. B., Lloyd, P. F., Bunning, T. J., and Huang, T. J., 2007, "Aminopropyltriethoxysilane (APTES)-Functionalized Nanoporous Polymeric Gratings: Fabrication and Application in Biosensing," *J. Mater. Chem.*, **17**, pp. 4896–4901.
- [34] Shi, J., Hsiao, V. K. S., and Huang, T. J., 2007, "Nanoporous Polymeric Transmission Gratings for High-Speed Humidity Sensing," *Nanotechnology*, **18**, p. 465501.
- [35] Yan, W., Hsiao, V. K. S., Zheng, Y. B., Shariff, Y. M., Gao, T., and Huang, T. J., 2009, "Towards Nanoporous Polymer Thin Film-Based Drug Delivery Systems," *Thin Solid Films*, **517**, pp. 1794–1798.
- [36] Liu, Y. J., Dai, H. T., Sun, X. W., and Huang, T. J., 2009, "Electrically Switchable Phase-Type Fractal Zone Plates and Fractal Photon Sieves," *Opt. Express*, **17**, pp. 12418–12423.
- [37] Liu, Y. J., Zheng, Y. B., Shi, J., Huang, H., Walker, T. R., and Huang, T. J., 2009, "Optically Switchable Gratings Based on Azo-Dye-Doped, Polymer-Dispersed Liquid Crystals," *Opt. Lett.*, **34**, pp. 2351–2353.
- [38] Zheng, Y. B., Yang, Y. W., Jensen, L., Fang, L., Juluri, B. K., Flood, A. H., Weiss, P. S., Stoddart, J. F., and Huang, T. J., 2009, "Active Molecular Plasmonics: Controlling Plasmon Resonances With Molecular Switches," *Nano Lett.*, **9**(2), pp. 819–825.
- [39] Hsiao, V. K. S., Zheng, Y. B., Juluri, B. K., and Huang, T. J., 2008, "Light-Driven Plasmonic Switches Based on Au Nanodisk Arrays and Photoresponsive Liquid Crystals," *Adv. Mater.*, **20**(18), pp. 3528–3532.
- [40] Juluri, B. K., Lu, M., Zheng, Y. B., Huang, T. J., and Jensen, L., 2009, "Coupling Between Molecular and Plasmonic Resonances: Effect of Molecular Absorbance," *J. Phys. Chem. C*, **113**(43), pp. 18499–18503.
- [41] Juluri, B. K., Zheng, Y. B., Ahmed, D., Jensen, L., and Huang, T. J., 2008, "Effects of Geometry and Composition on Charge-Induced Plasmonic Shifts in Gold Nanoparticles," *J. Phys. Chem. C*, **112**(19), pp. 7309–7317.
- [42] Zheng, Y. B., Jensen, L., Yan, W., Walker, T. R., Juluri, B. K., Jensen, L., and Huang, T. J., 2009, "Chemically Tuning the Localized Surface Plasmon Resonances of Gold Nanostructure Arrays," *J. Phys. Chem. C*, **113**(17), pp. 7019–7024.
- [43] Zheng, Y. B., Juluri, B. K., Jensen, L. L., Ahmed, D., Lu, M., Jensen, L., and Huang, T. J., 2010, "Dynamically Tuning Plasmon-Exciton Coupling in Arrays of Nanodisk-J-Aggregate Complexes," *Adv. Mater.*, **22**, pp. 3603–3607.
- [44] Bunning, T. J., Natarajan, L. V., Tondiglia, V. P., and Sutherland, R. L., 2000, "Holographic Polymer-Dispersed Liquid Crystals," *Annu. Rev. Mater. Sci.*, **30**, pp. 83–115.
- [45] Natarajan, L. V., Brown, D. P., Wofford, J. M., Tondiglia, V. P., Sutherland, R. L., Lloyd, P. F., and Bunning, T. J., 2006, "Holographic Polymer Dispersed Liquid Crystal Reflection Gratings Formed by Visible Light Initiated Thiol-Ene Photopolymerization," *Polymer*, **47**(12), pp. 4411–4420.
- [46] Urbas, A., Tondiglia, V., Natarajan, L., Sutherland, R., Yu, H., Li, J.-H., and Bunning, T., 2004, "Optically Switchable Liquid Crystal Photonic Structures," *J. Am. Chem. Soc.*, **126**, pp. 13580–13581.
- [47] Bunning, T. J., Natarajan, L. V., Tondiglia, V. P., Sutherland, R. L., Vezie, D. L., and Adams, W. W., 2006, "Morphology of Reflection Holograms Formed In-Situ Using Polymer-Dispersed Liquid Crystals," *Polymer*, **37**(14), pp. 3147–3150.